

Characterization of low-frequency noise in molecular beam epitaxy-grown GaN epilayers deposited on double buffer layers

W. K. Fong,^{a)} S. W. Ng, B. H. Leung, and Charles Surya
*Department of Electronic and Information Engineering and Photonics Research Center,
The Hong Kong Polytechnic University, Hong Kong*

(Received 3 December 2002; accepted 14 April 2003)

We report the growth of high-mobility Si-doped GaN epilayers utilizing unique double buffer layer (DBL) structures, which consist of a thin buffer layer and a thick GaN intermediate-temperature buffer layer (ITBL). In this study, three types of DBL were investigated: (i) thin GaN low-temperature buffer layer /GaN ITBL (type I); (ii) nitridated Ga metal film/GaN ITBL (type II); and (iii) thin AlN high-temperature buffer layer /GaN ITBL (type III). Systematic measurements were conducted on the electron mobilities and the low-frequency noise over a wide range of temperatures. It is found that the electron mobilities of the GaN films are substantially improved with the use of DBLs, with the sample using type III DBL which exhibits the highest low-temperature mobility. Furthermore, the same sample also demonstrates the elimination of deep levels at 91 and 255 meV below the conduction band. This is believed to result from the relaxation of tensile stress during growth with the use of type III DBLs. © 2003 American Institute of Physics. [DOI: 10.1063/1.1579843]

INTRODUCTION

Lacking a commercial native substrate, (0001) oriented sapphire wafers are commonly used for the growth of GaN thin films. Heteroepitaxial growth of GaN films on sapphire substrates results in stress and high defect density in the epilayers due to the large mismatches in the lattice constants and the coefficients of thermal expansion between sapphire and GaN. In such strongly lattice mismatched systems, the growth of high-quality GaN films requires the deposition of a buffer layer between the GaN epilayer and the substrate at a relatively low temperature to provide a high-density of nucleation centers. It was found that the AlN or GaN low-temperature buffer layer serves to enhance two-dimensional growth and the density of nucleation for the epitaxial films due to the reduction in the interfacial energy for the GaN/buffer system compared to the GaN/sapphire system. The use of a thin AlN or GaN low-temperature buffer layer is highly effective in the improvement of GaN film quality deposited by the metalorganic chemical vapor deposition (MOCVD) technique.^{1–4} However, this technique has achieved limited success in molecular beam epitaxy (MBE) process. To date, MOCVD-grown GaN films are superior to the MBE-grown counterparts. Nevertheless, the MBE growth technique does have a number of advantages, particularly in the growth of the modulation doped structure and solar-blind UV detectors.⁵ It is therefore important to investigate the optimization of the growth parameters for improving the quality of MBE-grown GaN films. The authors have recently reported on MBE growth of high-quality GaN layers on novel double buffer layer (DBL) structures, which consist of a thin GaN low-temperature buffer layer (LTBL) and a thick GaN

intermediate-temperature buffer layer (ITBL) deposited at 500 and 690 °C, respectively. It was shown that the use of the DBL resulted in substantial improvements in both the optical and electronic properties arising from strain relaxation of the top GaN epitaxial film during the epitaxial growth process.^{6–9} It has also been reported that the growth conditions of the thin buffer layer (TBL) may affect the quality of the ITBL grown on top, which, in turn, will have significant impact on the quality of the top epitaxial layer.^{6,7}

In this article, detailed studies were performed to investigate the effect of different DBL systems on the quality of the GaN epilayers. Investigations on the electronic and optical characteristics of the films will be presented and, in particular, we will report detailed studies of the low-frequency noise characteristics measured from the materials.

EXPERIMENT

High-mobility Si-doped GaN thin films were grown on (0001) sapphire substrates by rf plasma-assisted MBE equipped with an Applied-EPI UNI-Bulb nitrogen plasma source. The substrate temperature was measured by a two-color pyrometer, which was calibrated with the Al melting point. Two inch sapphire substrates were cleaned by organic solvents, followed by etching in 3H₂SO₄:1H₃PO₄ solution at 120 °C for 20 min. The substrates were then rinsed in de-ionized water and blown dry with filtered nitrogen gas. After cleaning, the sapphire wafers were transferred to the growth chamber where they were outgassed at 850 °C for 30 min. Nitridation was then performed at 500 °C for 20 min with nitrogen flow rate of 1.0 sccm and a rf power of 500 W. Subsequently, the TBLs were grown followed by the deposition of 800 nm GaN ITBLs at 690 °C. Three different types of TBLs were studied: (i) 20-nm-thick GaN grown at 500 °C (type I); (ii) thin metallic Ga deposited at 500 °C followed by

^{a)} Author to whom correspondence should be addressed; electronic mail: enwkfong@polyu.edu.hk

a nitridation process under nitrogen plasma during substrate temperature ramping to the main growth temperature of 740 °C (type II); and (iii) 20-nm-thick AlN grown at 750 °C (type III). Finally, Si-doped GaN epilayers were grown on top of the DBLs at 740 °C. The thickness and the carrier concentration of the Si-doped GaN epilayer were 1.8 μm and $3 \times 10^{17} \text{ cm}^{-3}$, respectively. The surface morphology and the optimal III/V ratio were monitored *in situ* by reflection high-energy electron diffraction pattern.

Temperature dependent Hall-coefficient measurements were conducted in a custom-made system over a temperature range from 90 to 300 K. Room-temperature Hall-effect measurements were also carried out in a BioRad HL5500 system. The magnetic field was 0.33 T and the current bias was 0.1 mA. Both Van der Pauw and cross-bridge resistive structures were used for the Hall measurements. Details of the fabrication process of the cross-bridge resistive structure can be found elsewhere.^{10–12} The contact resistance was monitored by the I – V characteristics during the Hall-effect measurement. It must be stressed that excellent uniformity and reproducibility of the results were observed in our devices. For example, the measured carrier mobilities recorded from five different samples grown on type I DBLs under the same growth conditions were within the range $377 \pm 12 \text{ cm}^2 \text{ V}^{-1} \text{ s}^{-1}$. To minimize the experimental error, all samples were cut from the center region of the 2 in. wafers. It is noted that Hall-effect measurements on the samples grown on type III DBL were done on Van der Pauw geometry only because these samples are Ga-faced, which are KOH resistant. Hereafter, samples grown on types I, II, and III DBL are referred to as samples I, II, and III, respectively. Variations in the residual strain in the GaN epitaxial layers were determined from the changes in the band edge position of the room-temperature photoluminescence (PL). Details of the PL setup is found in previous reports.^{6,7,9}

Detailed investigations on the low-frequency noise characteristics were conducted on the samples over a wide range of temperatures. Interdigitated devices were fabricated by sputter deposition of Ti/Al (30 nm/70 nm) bilayers on samples I, II, and III. The metallic fingers were fabricated using a self-aligned technique. The fingers are 2 μm wide and the finger spacing is 10 μm . The devices were placed inside a continuous flow cryostat and were current biased by a passive current source with an output resistance at least 30 times that of the device under test. The temperatures of the devices were controlled using a Lakeshore 91C temperature controller. The fluctuating voltages across the devices were amplified by 10^4 times using a PAR 113 low-noise pre-amplifier and was then ac coupled to an HP 3561A dynamic signal analyzer for the measurement of voltage noise power spectra. Details of the noise measurement can be found in previous publications.^{13,14}

RESULTS AND DISCUSSION

The temperature dependencies of the measured Hall mobility, μ_H , for GaN films grown on types I (diamond), II (square), and III (triangle) DBL are shown in Fig. 1. Significant improvements in the electron mobilities are observed.

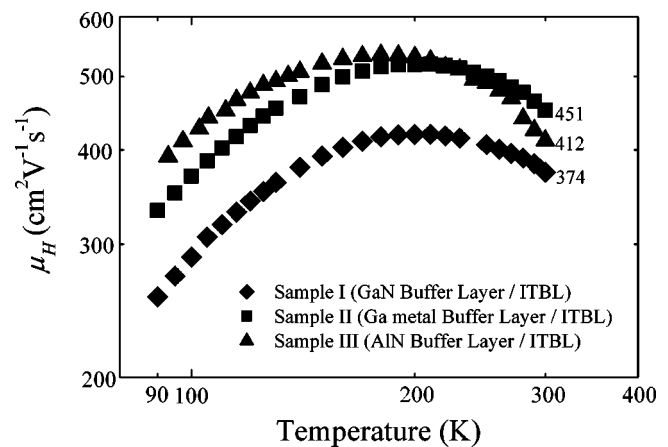


FIG. 1. Temperature dependent Hall mobility of samples grown on different double buffer layer structures in log–log scale.

Room temperature Hall mobilities of samples I, II, and III are 374, 451, and 412 $\text{cm}^2 \text{ V}^{-1} \text{ s}^{-1}$, respectively. In previous publications,^{7,8,15} the authors have shown that the utilization of type I DBL significantly improves the Hall mobility by a factor of 4.5 times compared to the control device, which was grown on a single GaN LTBL. As shown in Fig. 1, all samples go through a maximum mobility at about 200 K, indicating that the mobility is dominated by polar phonon scattering for $T > 200 \text{ K}$, while it is dominated by ionized impurity scattering at $T < 200 \text{ K}$. The mobility associated with polar phonon scattering has a temperature dependence of T^x with $x = -1.5$ and that associated with ionized impurity scattering has a temperature dependence of T^x with $x = 1.5$. The experimental data are fitted according to $\mu_H - T^x$ dependence. However, the power coefficient, x , of all samples deviated from 1.5 which is attributed to some other scattering mechanisms such as piezoelectric field, residual strain, and charged dislocations in the epilayers, which are commonly observed in GaN films grown on highly lattice mismatched substrates.

The improvement in the Hall mobility is attributed to the relaxation of the residual strain in the top epilayers during the growth process. The room-temperature Hall mobilities obtained in the samples are outstanding values compared with other reported values for strictly rf-plasma MBE-grown GaN films on sapphire substrates. It is noteworthy that a room-temperature mobility of 451 $\text{cm}^2 \text{ V}^{-1} \text{ s}^{-1}$ is obtained when the conventional TBL is replaced by a nitridated Ga metal film. Initial studies by Kim *et al.*^{16,17} have elucidated on the physical processes that underlie the elastic strain relief in nitridated Ga metal buffer layer for the heteroepitaxial growth of GaN. A maximum mobility of 400 $\text{cm}^2 \text{ V}^{-1} \text{ s}^{-1}$ was obtained by Kim *et al.* utilizing nitridated Ga metal buffer layer. The results obtained in our samples represent a further improvement on the mobility obtained by Kim *et al.*, indicative of better film quality when utilizing type II DBL. The experimental results indicate that type II DBL has the potential in further improving the crystallinity of the epilayer. It was suggested by Kim *et al.* that the improved mobility may arise from the unreacted Ga metal, which serves as a compliant buffer layer for heteroepitaxy. It was found

that the fraction of stress transferred from substrate to epilayer was as low as 27% for samples grown on nitridated metal buffer layers, compared to nearly 100% for samples grown on conventional GaN LTBLs.¹⁶ We speculate that the unreacted metallic Ga may have softened and yielded plastically leading to the reduction in the strain and the dislocation density both in the ITBL and the top epitaxial layers.

A dislocation model had been proposed by Weimann *et al.*¹⁸ to account for the low electron mobility in GaN epilayers. The model takes into the consideration that negatively charged threading dislocations with an edge component act as Coulomb scattering centers. This scattering mechanism becomes the dominant one at doping levels equivalent with the volume concentration of traps introduced by dislocations. The dislocation density determined from this model was proved to be in good agreement with transmission electron microscopy (TEM) results.^{19,20} Based on the dislocation model, the dislocation densities of samples I and III are estimated to be mid- 10^9 cm^{-2} whereas sample II is in the low- 10^9 cm^{-2} range. Future works on TEM and selective photoenhanced wet etching²¹ experiments will be done to further elucidate the effects of types I, II, and III DBL on the reduction in dislocation density and this will be subject of a separate publication.

Both samples I and II are found to be N faced as confirmed by a hot KOH etch test. Typically, MOCVD- or HVPE-grown GaN films are Ga-faced whereas MBE-grown GaN films are N faced when using GaN buffer layer. In order to grow Ga-faced GaN films by MBE, AlN buffer layer is used.²² As discussed earlier, the relation between the carrier mobility and the dislocation density of the GaN films can be explained by the proposed dislocation model.¹⁸ However, the relation between the polarity of GaN film and carrier mobility (or dislocation density) is still not certain to date.²³ It is well known that Ga-faced GaN has superior surface morphology compared to N-faced GaN. Realization of Ga-faced GaN films grown by MBE is expected to lead to important applications in GaN-based optoelectronic devices. Sample III is shown to be Ga-faced based on the results on KOH etch test. It must be stressed that the improved carrier mobility in samples II and III compared to sample I cannot simply be explained by a change in the free carrier concentration alone since it is constant at $\sim 3 \times 10^{17}$ cm^{-3} for all samples being studied.

The room-temperature PL spectra of the samples are shown in Fig. 2. It is observed that the intensities of the band edge emission of samples II and III are nearly doubled that of sample I. It is also noted that yellow-band emission, commonly seen in both doped and undoped GaN, cannot be detected from our samples which means that it is at least three orders of magnitude, the detection limit of our PL system, below the band edge emission. It is widely accepted that the yellow emission arises from Ga vacancy in the material. Thus, the improvements in the optical quality of the films clearly demonstrates improvements in the defect properties of the GaN films grown with the utilization of DBLs.

A number of authors have shown that the relaxation of the residual strain is associated with the shift in the PL and photoreflectance (PR) peak positions.^{24–26} The excitonic

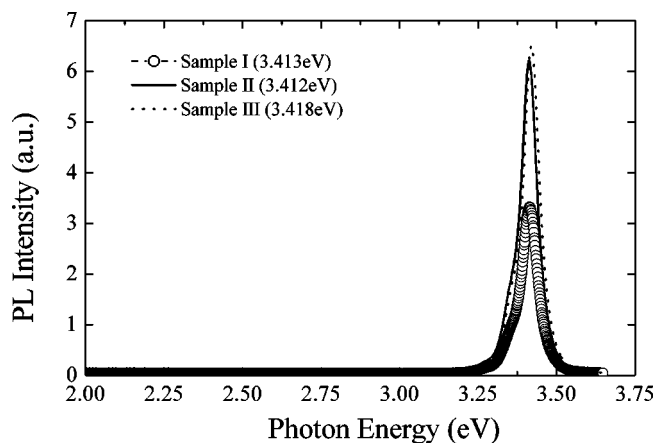


FIG. 2. Room temperature photoluminescence spectra of samples grown on different double buffer layer structures.

transition energy increases under compressive biaxial stress whereas it decreases under tensile biaxial stress. In our previous publications,^{7,8} detailed analyses of PL had shown that type I DBL can effectively reduce residual strain of the epilayer. In addition, PR experiments were conducted to further confirm the effect of ITBL on residual strain in the *n*-type GaN epilayers because experimental PR spectra are composed of derivative features which are often more pronounced than those obtained by direct reflectance. Because of its derivative character, it yields very sharp spectral features near the critical points of the band structure allowing the estimation of important parameters such as excitonic transition energy and thermal boardening. It is also stressed that PR is only concerned with free excitons, rather than with localized excitons or excitons complexes, in contrast to PL. In our previous publications^{7,8} it was found that the change in residual strain as a function of ITBL thickness determined from PL results were in good agreement with PR results.

In this article, the variations in residual strain in samples I, II, and III are determined from the shifts in the position of the band edge emission of the room-temperature PL. The room-temperature band gap energy of unstrained GaN is 3.39 eV. As shown in Fig. 2, the PL peak positions are 3.413, 3.412, and 3.418 eV for samples I, II, and III, respectively, indicating that sample III suffers from a large compressive stress compared to samples I and II. It was shown by Hearne *et al.*²⁷ that for GaN films grown pseudomorphically under tensile stress on sapphire substrates, the plastic deformation in the films is negligible during postgrowth cooling and dislocations in GaN have low mobility so that the dislocations freeze out after the epitaxial growth.²⁸ Due to the difference in thermal expansion coefficients between sapphire and GaN, it is postulated that larger compressive stress measured at room temperature corresponds to a lower tensile stress at the growth temperature as shown in Fig. 3. Thus, relative to samples I and II, sample III is expected to be grown under a smaller tensile stress at 740 °C. This has a significant implication on the growth mechanism of the film. It is well known that stress affects the adatom mobility during heteroepitaxial growth.²⁹ Compressive stress promotes adatoms surface diffusion whereas tensile stress increases the activation barrier.

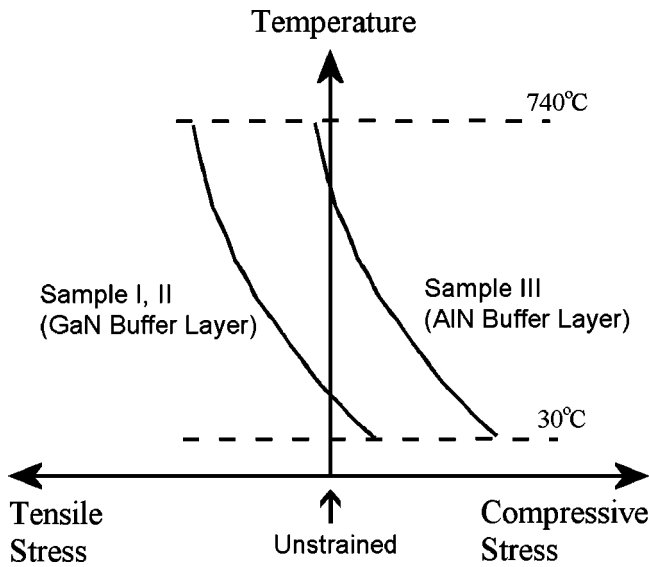


FIG. 3. A hypothesis that describes the reduced tensile stress during growth when using a double buffer layer structure.

Therefore, the formation of point defects and/or dislocations is reduced for sample III because of the enhanced Ga surface mobility during growth. For sample II, the shift in band edge emission relative to sample I is negligible which is not expected. It is because the incomplete coverage of nitridated Ga metal that leads to nonuniformity in the film.¹⁷ It is noteworthy that from the experimental data on the electron mobility we observe that while sample III records lower room-temperature mobility compared to sample II, it has the highest mobility of the three samples at low temperature. This is consistent with the model presented earlier since the PL results indicate that sample III has the highest room temperature compressive stress. This corresponds to a lower tensile stress at the growth temperature leading to improved two-dimensional growth for sample III. As a result the sample will exhibit higher scattering rate due to residual strain at room temperature but lower impurity scattering rate at low temperature compared to the other samples.

Low-frequency noise characteristics of the devices were investigated over a broad range of temperatures. In addition to being an important figure-of-merit for the devices, it represents the lowest signal that can be processed by the device. It has been shown that the noise characteristics can be utilized as a powerful tool for material quality characterization. This is because the voltage noise power spectral density for a resistive device is given by

$$S_V(f) = 4 \int_x \int_y \int_z \int_E N_T(x, y, z, E) f_T(1 - f_T) \times \frac{\tau}{1 + \omega^2 \tau^2} dx dy dz dE, \quad (1)$$

where N_T is the trap density in the material. Equation (1) stipulates that the voltage noise power spectral density is directly proportional to the trap density.

Typical room-temperature voltage noise power spectra, $S_V(f)$, are shown in Fig. 4 which exhibit a typical spectral

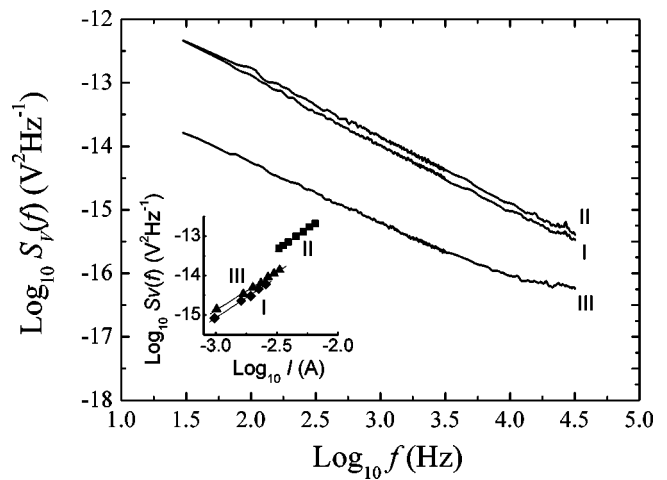


FIG. 4. Room temperature $S_V(f)$ of GaN films on different types of double buffer layer structure. The inset shows the bias dependence of $S_V(f)$.

form of $1/f^\gamma$ with $\gamma \approx 1$. Substantial reduction in $S_V(f)$ for sample III is clearly observed, indicative of the corresponding reduction in the trap density. Our experimental results demonstrate excellent repeatability. The standard deviation of the voltage noise power spectral densities measured from five different devices was found to be within 3 dB. Typical current dependence exhibits roughly a quadratic relationship with the bias current as shown in the inset of Fig. 4, indicative that flicker noise does not originate from the metal contacts or other extraneous sources.³⁰ At reduced temperatures, the experimental results on the low-frequency noise show that the voltage noise power spectra exhibit superposition of $1/f$ noise and Lorentzian bumps originating from generation-recombination ($G-R$) process. The results show that cutoff frequencies of the Lorentzians, f_0 , are strongly temperature dependent, from which the fluctuation time constants can be determined experimentally by $\tau = 1/2\pi f_0$. The $G-R$ noise is modeled by thermally activated capture and emission processes with $\tau = \tau_0 \exp(E_\tau/kT)$ where E_τ is the trap thermal activation energy. The experimental values for E_τ can be determined from the Arrhenius plot of τ (Ref. 31) as shown in Fig. 5. For samples I and II, deep levels at 255 and 91 meV are observed. Similar results were reported on N-faced

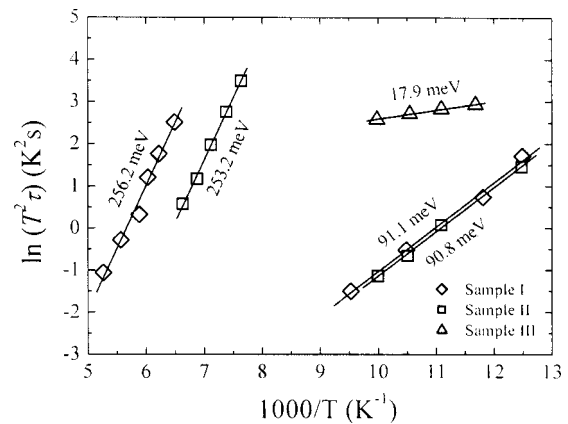


FIG. 5. Arrhenius plots of the fluctuation time constant, τ , for samples grown on different types of double buffer layer structure.

GaN films grown on ITBL.¹³ It is interesting to note that only one type of $G-R$ levels at 17.9 meV is observed in sample III and are substantially lower than those observed in samples I and II. To investigate the origin of the centers we note that the Arrhenius plots of the carrier concentration based on the low-temperature Hall results yielded an activation energy for the Si dopants in the range of 25–27 meV. To take screening effect into consideration it was noted by Götz *et al.*³² that the activated energy obtained from the Arrhenius analysis yields $\sim 4/3$ of the actual activation energy of the dopant. Thus, the screened donor activation energy for our samples are about 19–20 meV. This is in good agreement with the activation energy we obtained from the $G-R$ bumps in the voltage noise power spectra for sample III, strongly indicating that the $G-R$ bumps obtained from the sample originate from the Si donor atoms in the films. The results indicate that the use of type III DBL leads to the elimination of the deep levels. The physical nature of the deep levels, other than the activation energy, is not certain to date because it cannot be determined based on low-frequency noise measurement alone. In general, it is assumed that these deep levels arise from crystalline defects or impurities.

CONCLUSION

In summary, Si-doped GaN films were grown on double buffer layer structures, which consist of a thin buffer layer and a GaN intermediate-temperature buffer layer of thickness 800 nm. Three different types of thin buffer layers were investigated: (i) low-temperature GaN layer; (ii) nitridated metallic Ga layer; and (iii) high-temperature AlN layer. Gallium-faced GaN epilayers can be obtained using a high-temperature AlN thin buffer layer. All samples grown on double buffer layers demonstrate enhanced Hall mobility with a maximum mobility of $520 \text{ cm}^2 \text{ V}^{-1} \text{ s}^{-1}$ at around 200 K for the film deposited utilizing an AlN thin buffer layer. Room-temperature photoluminescence measurements were performed to determine the residual strain in the top epilayer. Our results demonstrate that the use of a double buffer layer structure, consisting of an AlN thin buffer layer/GaN intermediate-temperature buffer layer, leads to the reduction in tensile stress at the growth temperature and thereby reduces the activation barrier of adatoms surface diffusion. Low-frequency noise results also reveal that the use of AlN thin buffer layer is effective in the elimination of deep levels at energies 91 and 255 meV below the conduction band.

ACKNOWLEDGMENTS

This work was supported in part by grants from the Research Grants Council of the Hong Kong Special Adminis-

trative Region, China (Project Nos. CRC 4/98 and PolyU5098/98E) and a university research grant from The Hong Kong Polytechnic University.

- ¹S. Yoshida, S. Misawa, and S. Gonda, *Appl. Phys. Lett.* **42**, 427 (1983).
- ²I. Akasaki, H. Amano, K. Hiramatsu, and N. Sawaki, *J. Cryst. Growth* **98**, 209 (1989).
- ³J. N. Kuznia, M. A. Khan, D. T. Olson, R. Kaplan, and J. Freitas, *J. Appl. Phys.* **73**, 4700 (1993).
- ⁴S. Nakamura, *Jpn. J. Appl. Phys., Part 2* **30**, L1705 (1991).
- ⁵H. Z. Xu, Z. G. Wang, M. Kawabe, I. Harrison, B. J. Ansell, and C. T. Foxon, *J. Cryst. Growth* **218**, 1 (2000).
- ⁶W. K. Fong, C. F. Zhu, B. H. Leung, and C. Surya, *MRS Internet J. Nitride Semicond. Res.* **5**, 12 (2000).
- ⁷W. K. Fong, C. F. Zhu, B. H. Leung, and C. Surya, *J. Cryst. Growth* **233**, 431 (2001).
- ⁸C. F. Zhu, W. K. Fong, B. H. Leung, and C. Surya, *Appl. Phys. A: Mater. Sci. Process.* **A72**, 495 (2001).
- ⁹B. H. Leung, W. K. Fong, C. F. Zhu, and C. Surya, *IEEE Trans. Electron Devices* **48**, 2400 (2001).
- ¹⁰B. H. Leung, W. K. Fong, C. F. Zhu, and C. Surya, *J. Appl. Phys.* **91**, 3706 (2002).
- ¹¹C. F. Zhu, W. K. Fong, B. H. Leung, C. C. Cheng, and C. Surya, *IEEE Trans. Electron Devices* **48**, 1225 (2001).
- ¹²C. Surya, C. F. Zhu, B. H. Leung, W. K. Fong, C. C. Cheng, and J. K. O. Sin, *Microelectron. Reliab.* **40**, 1905 (2000).
- ¹³J. Q. Xie, W. K. Fong, B. H. Leung, C. F. Zhu, and C. Surya, *Fluct. Noise Lett.* **1**, R163 (2001).
- ¹⁴B. H. Leung *et al.*, *IEEE Trans. Electron Devices* **49**, 314 (2002).
- ¹⁵W. K. Fong, B. H. Leung, C. F. Zhu, and C. Surya, *Mater. Res. Soc. Symp. Proc.* **693**, I3.38.1 (2002).
- ¹⁶K. Kim, N. A. Shapiro, H. Feick, R. Armitage, E. R. Weber, Y. Yang, and F. Cerrina, *Appl. Phys. Lett.* **78**, 895 (2001).
- ¹⁷Y. Kim *et al.*, *Mater. Res. Soc. Symp. Proc.* **622**, T4.10.1 (2000).
- ¹⁸N. G. Weimann, L. F. Eastman, D. Doppalapudi, H. M. Ng, and T. D. Moustakas, *J. Appl. Phys.* **83**, 3656 (1998).
- ¹⁹H. M. Ng, D. Doppalapudi, T. D. Moustakas, N. G. Weimann, and L. F. Eastman, *Appl. Phys. Lett.* **73**, 821 (1998).
- ²⁰D. Sugihara, A. Kikuchi, K. Kusakabe, S. Nakamura, Y. Toyoura, T. Yamada, and K. Kishino, *Jpn. J. Appl. Phys., Part 2* **39**, L197 (2000).
- ²¹C. Youtsey, L. T. Romano, R. J. Molnar, and I. Adesida, *Appl. Phys. Lett.* **74**, 3537 (1999).
- ²²X. Q. Shen, T. Ide, S. H. Cho, M. Shimizu, S. Hara, H. Okumura, S. Sonoda, and S. Shimizu, *J. Cryst. Growth* **218**, 155 (2000).
- ²³E. S. Hellman, *MRS Internet J. Nitride Semicond. Res.* **3**, 11 (1998).
- ²⁴B. Gil, O. Briot, and R. L. Aulombard, *Phys. Rev. B* **52**, R17028 (1995).
- ²⁵C. Kieselowski *et al.*, *Phys. Rev. B* **54**, 17745 (1996).
- ²⁶W. Shan, R. J. Hauenstein, A. J. Fischer, J. J. Song, W. G. Perry, M. D. Bremser, R. F. Davis, and B. Goldenberg, *Phys. Rev. B* **54**, 13460 (1996).
- ²⁷S. Hearne, E. Chason, J. Han, J. A. Floro, J. Figiel, J. Hunter, H. Amano, and I. S. T. Tsong, *Appl. Phys. Lett.* **74**, 356 (1999).
- ²⁸L. Sugiura, *J. Appl. Phys.* **81**, 1633 (1997).
- ²⁹M. Schroeder and D. E. Wolf, *Surf. Sci.* **375**, 129 (1997).
- ³⁰P. V. Necliudov, S. L. Rumyantsev, M. S. Shur, D. J. Gundlach, and T. N. Jackson, *J. Appl. Phys.* **88**, 5395 (2000).
- ³¹F. N. Hooge, T. G. M. Kleinpenning, and L. K. J. Vandamme, *Rep. Prog. Phys.* **44**, 479 (1981).
- ³²W. Götz, N. M. Johnson, C. Chen, H. Liu, C. Kuo, and W. Imler, *Appl. Phys. Lett.* **68**, 3144 (1996).